2nd URSI AT-RASC, Gran Canaria, 28 May – 1 June 2018

Comparison Between a Multiband PIFA and a Ultrawideband Archimedean Spiral Antenna for Energy Harvesting in Microwave Bands

Antonio Alex-Amor [(1)], José M. Fernández-González [(1)], Pablo Padilla [(2)], and Manuel Sierra-Castañer [(1)]
(1) Technical University of Madrid, Madrid, Spain, e-mail: {aalex, jmfdez, m.sierra.castaner}@gr.ssr.upm.es;
(2) University of Granada, Granada, Spain; e-mail: pablopadilla@ugr.es

Abstract

This paper shows a comparison between a linearly-polarized multiband PIFA (Planar Inverted F-Antenna) and a circularly-polarized ultrawideband Archimedean spiral antenna, both designed to be low-cost RF harvesters and to capture the spectrum energy in the bands of interest (FM, DTT, LTE, GSM, WiFi and WiMAX). It is commented and demonstrated how the Archimedean spiral, which works between 0.4 GHz and 18 GHz, presents a better behavior in most of its radiation characteristics: efficiency, matching, depolarization losses, etc.; and it is more tolerant to slight variations in some of its parameters, as Monte Carlo simulations show. It also solves the interoperability problem of the antenna between different countries, where frequency assignment plans can vary.

1. Introduction

Energy harvesting is defined as the process of obtaining energy from external sources, such as wind, sunlight, heat or those radiofrequency (RF) signals that propagate through the air; which is later conveniently processed and stored in order to feed, in general, low-power electronic systems. The most common energy harvesting techniques [1] are based on the reuse of the sunlight; on the reuse of kinetic energy, through mechanic movements or deformations inside the device; on the reuse of thermal energy, through thermocouples that take advantage of the Seebeck effect; and on the capture of electromagnetic radiation.

When particularizing Energy Harvesting to radiofrequency, there are a few topics to consider when designing the radiating element. As the location of the incoming RF signals is unknown, the antennas must have a radiation pattern that resembles as much as possible to an omnidirectional one, so no spatial direction prevails. It is also important that the antenna has a high efficiency, in order to avoid losing part of the reduced incoming energy. The most studied and used kind of antenna for this purpose is the multiband antenna, an element that has multiple narrow-band resonances in the bands of interest (they are usually placed between 80 MHz and 5 GHz in the vast majority of countries). Multiband antennas are generally very resonant, with their bandwidth being so reduced that an external change (e.g. change in ambient temperature) or a small deviation in some of their design parameters can move their resonances out of the bands of interest. Neither they are interoperable between countries, where frequency assignment plans can be different. On the other hand, wideband antennas (Vivaldi, bowtie, spiral, wideband monopole, etc.) are more tolerant, and a small physical variation in any of its parameters can be neglected due to their large bandwidth.

2. Design and Simulation of the Multiband PIFA

The PIFA (Planar Inverted F-Antenna) is a type of printed antenna commonly used in mobile communications. It can be considered as a particularization of a half-wave patch, where its center (the electric field is null at the center of a λ/2 patch) is short-circuited to the ground plane. This technique is very smart and allows reducing the size of the PIFA to more than half ($\leq \lambda/4$) without degrading any of its parameters, which permits placing it in small spaces, as mobile phones. The antenna presents a low directivity (3 – 8 dBi) and a high efficiency (around 80 %), so, combined with some appropriate slots over its surface, it can be transformed into a multiband antenna. Nevertheless, it is linearly polarized and as we do not know the polarization of the incoming signals, the depolarization losses will be higher than in the case of a circularly-polarized antenna.

The design equation of the PIFA antenna is presented in [2] and has the form

$$L + W + W_s = \frac{\lambda_d}{4} \qquad (1).$$

where L is the length, W is the width, W_s the short-circuited stub width, and λ_d the operating wavelength of the PIFA antenna. Note that reducing W_s permits us reducing the size of the antenna (L, W) , but the lower the stub width, the lower the antenna bandwidth (~8 %). If we design the PIFA to resonate at 930 MHz (without any dielectric, in order to reduce losses), and we assume a stub width of W_s=7 mm and a relation width-length $\frac{W}{L} = 0.95$, the length and the width of the PIFA must be $L = 44.9$ mm and $W = 42.7$ mm, respectively.

As commented before, the RF harvester must cover LTE (800, 2100, 2600 MHz), GSM (900, 1800 MHz) and WiFi (2400, 5200 MHz) bands because most of the useful energy in the radio spectrum is ubicated there, but it is quite difficult to design a multiband antenna with more than three resonances. Based on this, we propose a design where two different PIFAs are integrated in the same ground plane (90 x 55 mm), which is fed with a single coaxial probe (SMA connector) through a distribution network printed in a FR4 substrate ($\varepsilon_r = 4.7, \tan\delta = 0.014$ @ 1 MHz) and situated below the ground plane, as shown in Figure 1. Two metallic vias cross the structure, from the end of the distribution network to the feed points in both PIFAs, in order to feed the antenna. As mentioned in Figure 1(a), the PIFA placed on the right side of the image covers all GSM bands, while the other covers LTE-2100, WiFi, and LTE-2600 bands.

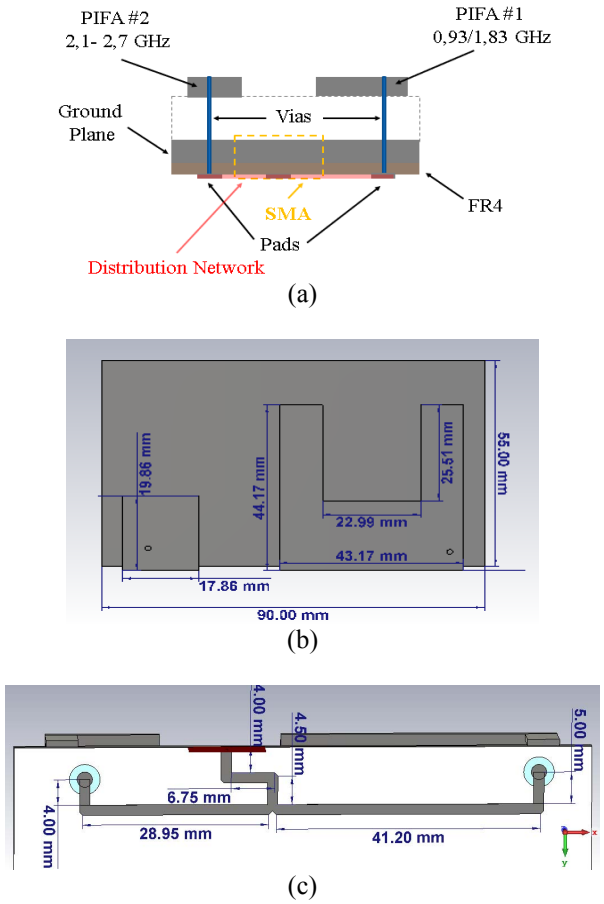

Figure 1. Transversal cut of the proposed multiband PIFA (a) and its top (b) and bottom (c) planes.

In Figure 2, it is presented a Monte Carlo simulation of the reflection coefficient in the proposed multiband antenna, where the inclination of the plane of both PIFAs has set to move in a range of $\pm 2^{\circ}$. The purple thick line represents the ideal scenario (null inclination). Note that there are four resonances in Figure 2: the first of them caused by PIFA #1; the second one (1450 MHz) caused by a parasitic resonance either of the ground plane or the metallic vias or

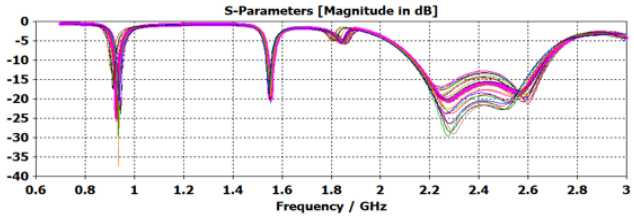

Figure 2. Monte Carlo simulation on the reflection coefficient of the proposed multiband antenna when varying the inclination of the plane of both PIFAs $\pm 2^{\circ}$.

the distribution network; the third one (1830 MHz) caused by an appropriate cut in PIFA #1; and the fourth one (2100-2700 MHz) caused by a resonance of PIFA #2. As Figure 2 proves, a slight manufacturing deviation on the inclination of both PIFAs ($\leq 2^{\circ}$) may mismatch the element in the bands of interest, leaving the antenna inoperative.

Figure 3 shows the far field radiation pattern of the proposed antenna at different frequencies. As expected, the multiband PIFA presents a non-directive behavior. Its total efficiency varies along the frequency according to its radiation efficiency and the antenna matching, being on average in a 76 % (the maximum is ubicated at 930 MHz, with a 95 %, and the minimum at 1830 MHz, with a 55 %).

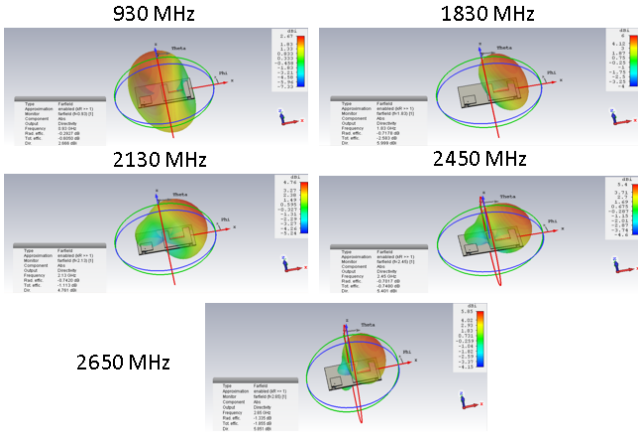

Figure 3. Far field radiation pattern of the proposed multiband antenna at different frequencies.

3. Design and Simulation of the Circularly-polarized Ultrawideband Archimedean Spiral Antenna

More than a ultrawideband antenna, the Archimedean spiral must be seen as a frequency independent one. According to Rumsey's principle [5], an antenna that is only defined by angles, as the Archimedean spiral or the equiangular spiral, shows an independent frequency behavior. In a self-complementary structure with an infinite length, the impedance (independent from frequency) of the antenna can be calculated as

$$Z_{ant}Z_{comp} = (60\,\pi)^2 \qquad (2).$$

where Z_{ant} is the impedance of our antenna and Z_{comp} the impedance of its complement. In the case of the Archimedean spiral antenna, $Z_{ant} = Z_{comp} = 60\,\pi\,\Omega \approx 188.5\,\Omega$. As expected, the finite size of the spiral will cause an imbalance with respect to this theoretical value. Several studies [6,7] point out that the Archimedean spiral antenna offers circular polarization, which is interesting in order to reduce depolarization losses, and that the current distribution over its surface tends to close to the center of the spiral at high frequencies (to the inner radius r_1) and tends to open to the end of the antenna (the outer radius r_2) at low frequencies (check out the simulations made in Figure 4). Based on this, its size is approximated according to equations (2) and (3) by setting its frequency operating range, determined by the upper cutoff frequency f_H and lower cutoff frequency f_L.

$$r_1 = \frac{c_o}{2\pi f_H \sqrt{\varepsilon_{reff}}} \qquad (3).$$

$$r_2 = \frac{c_o}{2\pi f_L \sqrt{\varepsilon_{reff}}} \qquad (4).$$

The term $\frac{c_o}{\sqrt{\varepsilon_{reff}}}$ represents the speed of the wave that crosses the dielectric, where c_o is the speed of light in vacuum and ε_{reff} the relative effective permittivity of the dielectric (FR4: ε_r=4.7, tan δ=0.014 @ 1MHz). As no ground plane is used, it is really difficult to estimate in an accurate manner ε_{reff}, so it is taken $\frac{\varepsilon_r+1}{2} = 2.85$ as the best approximation to it.

Self-complementarity is only reachable if the metallic strip width, w, is equal to the separation between two adjacent strips, s, that is, $w = s$. Fixing the upper and lower cutoff frequencies as 18 GHz and 0.4 GHz, respectively, and applying (2) and (3), it was found that the inner radius must be $r_1 = 1.5$ mm and the outer radius $r_2 = 70.7$ mm. Note that these values are mainly indicative, since, as seen in Figure 4, not all the current distribution over the surface of the spiral is located at the center or at the end of the antenna. In fact, as will be seen later, equation (4) works in a worse manner than equation (3), due to the current distribution at low frequencies does not really move to the end of the antenna (Figure 4(b)), but to an intermediate strip. Therefore, the real value of r_2 will be higher than the one calculated in (4).

In Figure 5, it is presented the Archimedean spiral antenna, designed over single-sided FR4 copper clad (no ground plane). As can be noticed, the value of the inner radius is $r_1 = 1.20$ mm, similar to the calculated value in equation (3), but the outer radius is slightly higher, with a value of $r_2 = 97.5$ mm. On the other hand, the metallic strip width w and the gap s were estimated by numerical simulations, giving us a value of $w = s = 3.9$ mm.

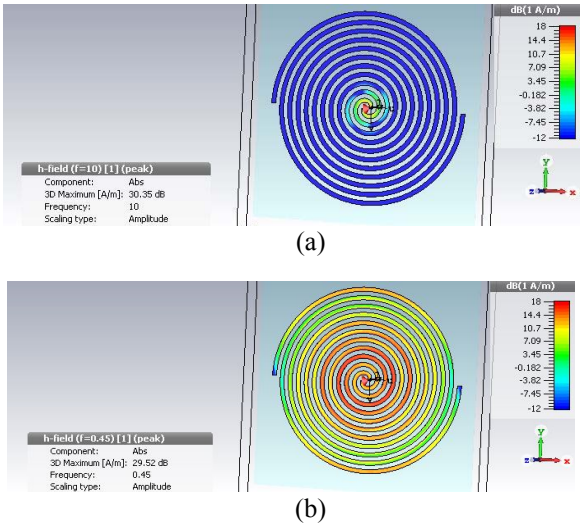

Figure 4. Current distribution over the Archimedean spiral antenna at (a) 10 GHz and (b) 450 MHz.

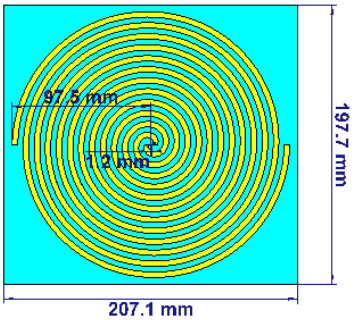

Figure 5. Archimedean spiral antenna.

Figure 6 shows the reflection coefficient of the Archimedean spiral antenna (normalized to 188.5 Ω). The antenna offers a bandwidth of 17.57 GHz ($|S_{11}| \leq -10$ dB), which ranges from 0.44 GHz to 18.01 GHz. It covers DTT (Digital Terrestrial Television), LTE, GSM, WiFi and WiMAX bands, and it is circularly polarized ($AR <$ 3 dB) in all bands but DTT, where this value is surpassed, as depicted in Figure 7. A ripple in the lower frequencies of the reflection coefficient is also observed, product of the short electrical size of the antenna. This means that the Archimedean spiral begins to show a resonant behavior and its impedance value is no longer constant at the lower frequencies.

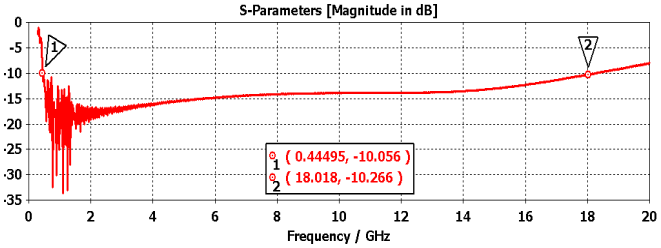

Figure 6. Reflection coefficient of the Archimedean spiral antenna (normalized to 188.5 Ω).

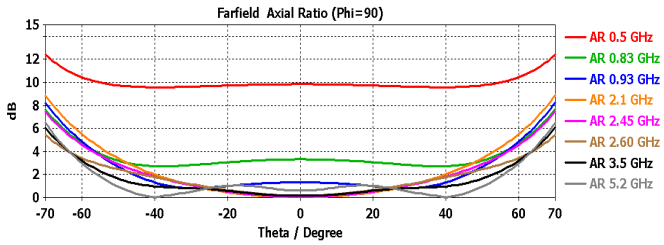

Figure 7. Axial ratio (AR) of the Archimedean spiral antenna at different frequencies in a cut in the plane $\boldsymbol{\varphi = 90º}$.

Finally, in Figure 8 and Figure 9, they are plotted the total efficiency and the far field radiation pattern of the Archimedean spiral antenna, respectively. As shown in Figure 8, the efficiency of the spiral is superior to 82% (0.82 if we normalize it to the unity) in the bands of interest, and the radiation pattern seems to be more homogeneous than in the case of the multiband antenna.

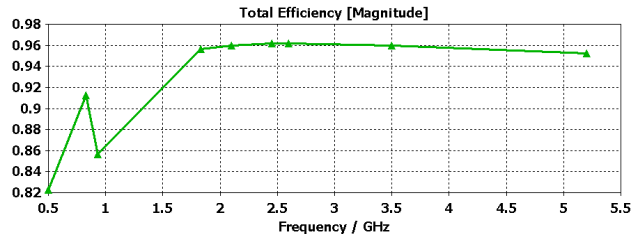

Figure 8. Total efficiency at different frequencies of the Archimedean spiral antenna.

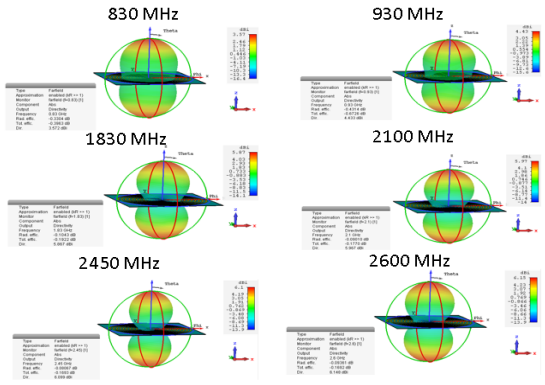

Figure 9. Far field radiation pattern at different frequencies of the Archimedean spiral antenna.

4. Conclusions

This paper presents a comparison between two types of antennas, a multiband and an ultrawideband antenna, oriented to be used in Energy Harvesting in RF. It was demonstrated how a slight manufacturing defect in the linearly-polarized multiband antenna can move some or their resonances and leave it inoperative in practice. On the other hand, the circularly-polarized Archimedean spiral antenna is posited as a better energy harvester, according to its easier design, better matching, efficiency, large bandwidth and circular polarization.

5. Acknowledgements

This work was supported by Madrid Regional Government under the project S2013/ICE-3000 (Space Debris Radar), and by Spanish Government under the project TEC2014-55735-C3-1-R (ENABLING5G). All simulations have been carried out using CST Studio Suite under a cooperation agreement between Computer Simulation Technology (CST) and Universidad Politécnica de Madrid.

6. References

1. L. Mateu and F. Moll, "Review of Energy Harvesting Techniques and Applications for Microelectronics" *Proceedings of the SPIE - The International Society for Optical Engineering*, 5837, June 2005.

2. K. Wong. "Planar Antennas for Wireless Communications". *John Wiley & Sons*, 2003.

3. A. Dadgarpour, A. Abbosh, and F. Jolani. "Planar Multiband Antenna for Compact Mobile Transceivers". *IEEE Antennas and Propagation Letters*, Vol. 10, pp. 651-654, 2011.

4. S. Al Ja'afreh, Y. Huang, L. Xing. "Low profile and wideband planar inverted-F antenna with polarization and pattern diversities". I*ET Microwaves, Antennas & Propagation*, 1751-8725, Aug. 2015.

5. V. H. Rumsey, "Frequency Independent Antennas". *IRE International Convention Record*, Vol. 5, March 1957, pp. 114-118.

6. E. D. Caswell. "Design and Analysis of Star Spiral with Application to Wideband Arrays with Variable Element Sizes" (Doctoral Thesis). Bradley Department of Electrical and Computer Engineering, Virginia Tech.

7. C.A. Balanis. "Antenna Theory. Analysis and Design". *John Wiley & Sons*, 3rd edition, 2005.

8. L. Tran, H. Cha, and W. Park. "RF Power Harvesting: a Review on Designing Methodologies and Applications". *Micro and Nano System Letters*, Feb. 2017.

9. S. Padmanathan, A. A. Al-Hadi, P. J. Soh, M. F. Jamlos. "A compact two-port tunable dual-band spiral antenna for MIMO terminals", *International Symposium on Antennas and Propagation (ISAP)*, 2017.

10. P. Liu, S. Yang, X. Wang, M. Yang, J. Song, and L. Dong. "Directivity-Reconfigurable Wideband Two-Arm Spiral Antenna", *IEEE Antennas and Wireless Propagation Letters,* 2017.